Cent. Eur. J. Phys. • 7(4) • 2009 • 762-767
DOI: 10.2478/s11534-009-0009-9

VERSITA

Central European Journal of **Physics**

DFT study on electronic structures and optical absorption properties of C, S cation- doped $SrTiO_3$

Research Article

Jiawen Liu[1]*, Lu Wang[2], Jihong Liu[1], Tianchi Wang[1], Weili Qu[1], Zhonghua Li[2]†

1 College of Chemistry and Chemical Engineering, Harbin Normal University, Harbin 150025, China

2 Harbin Institute of Technology, Harbin 150001, China

Received 13 November 2008; accepted 6 January 2009

Abstract: The effects of C cation and S cation doping on the electronic structures and optical properties of $SrTiO_3$ are investigated by density function theory (DFT) calculations. The calculated results reveal that the top of the valence band is predominately made up of the O 2p states for the pure $SrTiO_3$. When $SrTiO_3$ was doped with C cation and S cation, the top of the valence bands consists mainly of O 2p+C 2s hybrid orbitals and O 2p+S 3s hybrid orbitals, respectively. The band gap of $SrTiO_3$ is narrowed by the doping with C cation and S cation, especially for the C and S-codoped $SrTiO_3$. Moreover, the red shifts of the absorption edge are found by the calculated optical properties, which is consistent with reported experiment results. It is the explanation for their visible light respondency by the presence of C 2s and S 3s states on the upper edge of the valence band. All of these results can explain the good photocatalytic properties of C, S cation-codoped $SrTiO_3$ under visible light irradiation.

PACS (2008): 70.; 71.; 71.22.+i

Keywords: electronic structure • optical properties • $SrTiO_3$

1. Introduction

Photocatalysis is a technique that has great potential for the conversion of photon energy into chemical energy and for the decomposition of pollutants in air or solution. There is a need for effective catalysts for degradation of pollutants and water splitting. Because of its effective photocatalysis and photostability [1, 2], titanium dioxide (TiO_2) has been used for various industrial applications, such as water or air purification [3], antibacterial agents [4], and self-cleaning surfaces [5]. In addition to TiO_2, other metal oxides such as ZnO, Ta_2O_5, and $SrTiO_3$ have been reported as efficient photocatalysts [6–8]. Among these photocatalysts, $SrTiO_3$ has been used for water splitting and mineralization of organic pollutants under UV light irradiation [9–11]. However, their wide band gap (3.0–3.2 eV) requires UV light irradiation ($\lambda <$387 nm), that only utilizes about 3% of the solar energy available. Many studies have been conducted to improve the TiO_2 photocatalytic efficiency and extend the photosensitivity toward the visible light region to use natural solar energy [12–14] by means of the catalyst doping [15–17].

---

*E-mail: jwliu@hrbnu.edu.cn
†E-mail: lizh@hit.edu.cn

Recently, nonmetal-doped TiO_2 has become a rapidly growing field of interest [18–22]. N, S, or C anion-doped TiO_2 photocatalysts having an anatase form that show a relatively high level of activity under visible light irradiation have been reported [23–27]. Asahi *et al.* predicted by first-principle calculations and demonstrated in experiments that nitrogen-doped TiO_2 can lower its band gap and exhibit enhanced photoactivity under visible-light irradiation [23]. Recently, Wang *et al.* also reported an N-doped $SrTiO_3$ photocatalyst [28]. Teruhisa *et al.* also reported S, C cation-codoped $SrTiO_3$ and its photocatalytic activity under visible light [29]. After C and S ions were doped into $SrTiO_3$, the absorption edge of $SrTiO_3$ powder shifted greatly from 400 to 700 nm. Moreover, the photocatalytic activity of the doped $SrTiO_3$ was improved. Electronic band structures, density of states and optical properties have been reported for the large series of Strontium titanate modified crystals [30]. However, we have not found any report on electronic structures of nonmetal-doped $SrTiO_3$ semiconductor photocatalyst. It is necessary to understand the effects of different nonmetal doping on the electronic structures and photocatalytic properties of $SrTiO_3$.

In this paper, we calculated and compared the electronic structures of undoped, C cation - and S cation -doped $SrTiO_3$ by using DFT calculations. From these results, the photocatalytic properties of C, S cation -doped $SrTiO_3$ can be explained.

2. Computational details

The crystal structure of $SrTiO_3$ is cubic perovskite with the space group $Pm3m$, and the lattice constant is 0.3095 nm at room temperature. The Wyckoff positions of the atoms are: Sr 1*a* (0,0,0), Ti 1*b* (0.5,0.5,0.5) and O 3*c* (0.0,0.5,0.5). In our calculation, the electronic band-structure calculation was based on the CASTEP program [31]. The generalized gradient approximation (GGA) was adopted, an improvement of the local density approximation (LDA) within density functional theory [32–34] that is known to be an efficient and accurate scheme for solving the many-electron problem of a crystal. In the calculations, a 2×2×2 supercell was used in constructing the C, S cation-doped structures. To set the doped models, one titanium atom was replaced with a carbon atom and a sulfur atom for the C cation -doped and S cation-doped $SrTiO_3$ models, respectively. Two titanium atoms were replaced with a carbon atom and a sulfur atom for the C, S cation-codoped $SrTiO_3$ model, respectively. We used a 3×3×3 Monkhorst–Pack k-point mesh for the Brillouin Zone integration. A scissors operator of 1.32 eV was introduced to shift the conduction levels to be consistent with the measured value of the band gap [23, 35].

The absorption curves can be obtained from the imaginary part of the dielectric constant from the DFT calculation. The imaginary part of the dielectric constant is described as

$$\varepsilon_2(\hbar\omega) = \frac{2e^2}{\Omega\varepsilon_0}\sum_{c,v}\sum_{k}\left|\left\langle \Psi_k^c\middle|\hat{u}\cdot r\middle|\Psi_k^{\upsilon}\right\rangle\right|^2 \delta\left[E_k^c - E_k^{\upsilon} - \hbar\omega\right].$$

Where Ω is the volume of the elementary cell, k represents υ the k point, ω is the frequency of the incident light, c and υ represent the conduction and valence bands, respectively. Ψ_k^c and Ψ_k^{υ} are the eigenstates, $\mathbf{r}$ is the momentum operator, and $\hat{u}$ is the external field vector.

3. Results and discussion

3.1. Electronic structures

3.1.1. Density of states

In order to show the S, C doping effects on the electronic structure of $SrTiO_3$, the total density of states (TDOS) of each system were calculated and the results are shown in Fig. 1. From Fig. 1 we can see that the widths of the valence bands of C, S cation - doped $SrTiO_3$ are a little larger than that of undoped $SrTiO_3$ because of the C 2p and S 3p bands located in the nether part of the valence band. In addition, the VB and CB positions of C- and S-doped $SrTiO_3$ slightly shift compared with that of undoped $SrTiO_3$. For the C -doped $SrTiO_3$, the top of valence band and the bottom of conduction band slightly shift towards high energies. However, for the S -doped and C, S -codoped $SrTiO_3$, the band potentials slightly shift downwards. This indicates that VB of C, S-codoped $SrTiO_3$ should have a stronger oxidative power than that of undoped $SrTiO_3$. So it is reasonable that C, S cation-codoped $SrTiO_3$ shows a higher photocatalytic activity than undoped $SrTiO_3$ [36].

3.1.2. Partial density of states

To further analyze the S, C doping effects on the electronic structure of $SrTiO_3$, the partial density of states (PDOS) have been calculated, and the results are shown in Fig. 2a. The partial density of states of pure $SrTiO_3$suggest that the top of valence band is made up predominately of the O 2p states, and the bottom of conduction band has Ti 3d character. There is an energy gap between the occupied O 2p states and the unoccupied Ti 3d states. For the C- and S-doped $SrTiO_3$, the states in the valence

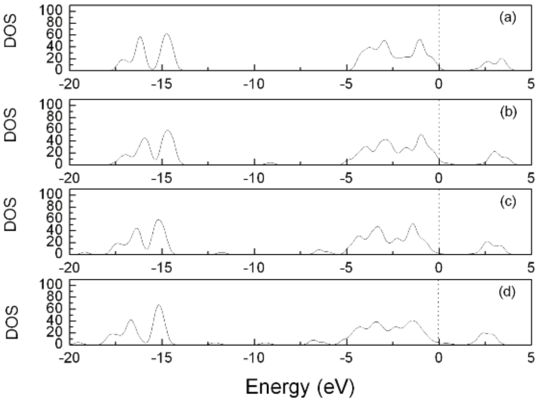

Figure 1. Calculated total density of states (DOS) of : (a) $SrTiO_3$, (b) C-doped $SrTiO_3$, (c) S-doped $SrTiO_3$, (d) C and S-codoped $SrTiO_3$.

band region mainly consist of the O 2p orbitals, but the contributions of C and S orbitals are not negligible. The top of valence band of the C-doped $SrTiO_3$ slightly shifts towards high energies by the presence of C 2s state localizing slightly above the upper edge of the valence band. In addition, for the C- and S-doped $SrTiO_3$, another small peak emerges above the lower VB at the energy of about -10 eV and -12.5 eV, in which C 2s and S 3s state make a great contribution, respectively. The conduction bands mainly consist of Ti 3d+C 2p orbitals for the C doping, and Ti 3d + S 3p orbitals for the S doping. For the C, S-codoped $SrTiO_3$, from the calculated results, we can find a similar variety. The conduction band mainly consists of Ti 3d+C 2p+S 3p orbitals.

There are three additional peaks between the upper VB and the lower VB. The three peaks are located at the bottom of the upper VB, above the lower VB and in the middle of the upper VB and the lower VB.

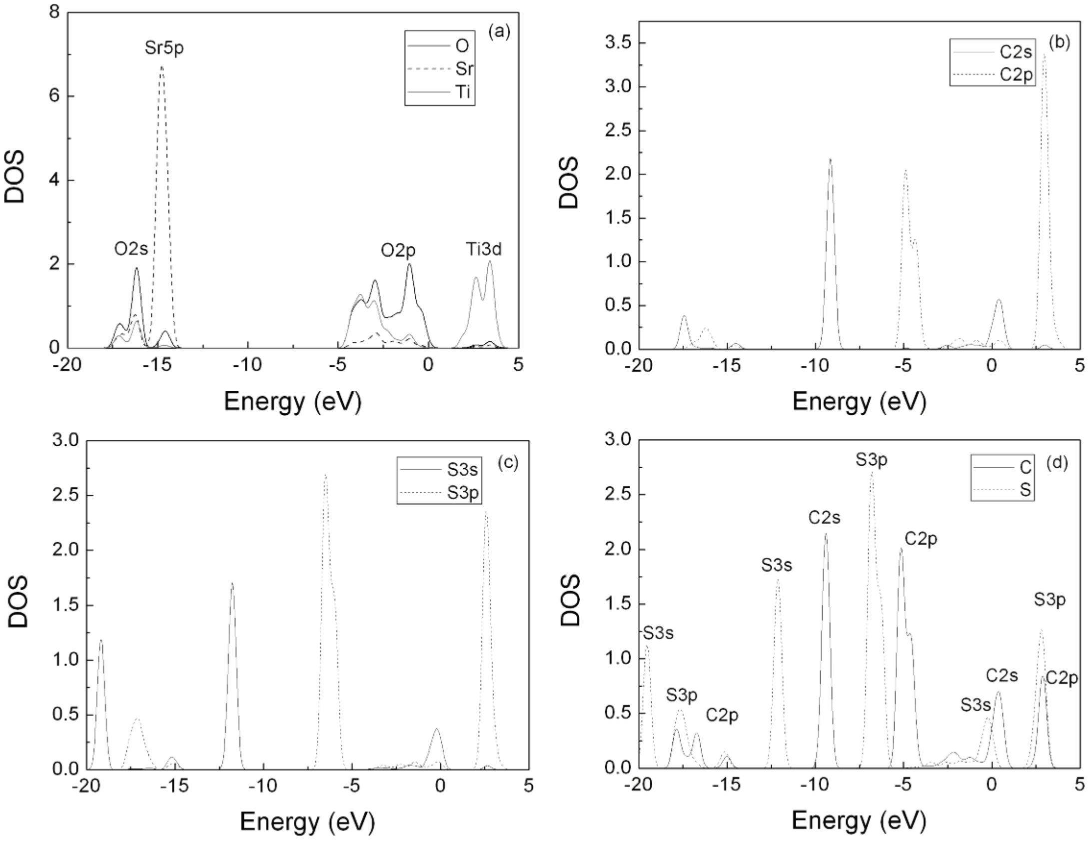

Figure 2. Partial density of states (PDOS) of undoped $SrTiO_3$ and doped $SrTiO_3$: (a) $SrTiO_3$, (b) PDOS of C in C-doped $SrTiO_3$, (c) PDOS of S in S-doped $SrTiO_3$, (d) PDOS of C,S in C and S-codoped $SrTiO_3$.

The contribution to the three peaks is S 3p+C 2p orbitals, S 3s orbitals and C 2s orbitals, respectively. The valence band mainly consists of the 2p orbitals of O atoms, mixed with some S 3s, C 2s and Ti 3d orbitals. There are some new states close to VB, and the contributions to the new states in the gap are derived from the mixture of S 3s, C 2s and O 2p orbitals. Excitations from the new states to a conduction band may be responsible for the red shift of the absorption edge observed in the C, S-codoped $SrTiO_3$ [36].

3.1.3. Band structures

The calculated energy band structure of each system is displayed in Fig 3a. As shown in Fig. 3a, the band-gap energy is about 1.88 eV for the pure $SrTiO_3$, which is an overly underestimated value compared with the experimental value of 3.2 eV [37, 38]. This underestimation comes from the inherent drawback of the GGA used for this calculation [39]. The calculated values however are acceptable for comparison. It is clear from this band structure that the band gap appears between the highest point of the valence band and the lowest point of the conduction band at the same G point. Therefore, a direct optical transition can occur. However, for the C-doped $SrTiO_3$ (Fig. 3b) and S-doped $SrTiO_3$ (Fig. 3c), the calculated band-gap energy is 1.52 eV and 1.72 eV, respectively. The band gaps show slight narrowing. Moreover, it indicates that C- and S -doped $SrTiO_3$ are all indirect band gap semiconductors with a minimum band gap between G and Q. Further analysis shows that the indirect band gap property is retained for the C, S -codoped $SrTiO_3$ and the band gap significantly becomes narrow due to C and S codoping. The band-gap energy is about 1.14 eV.

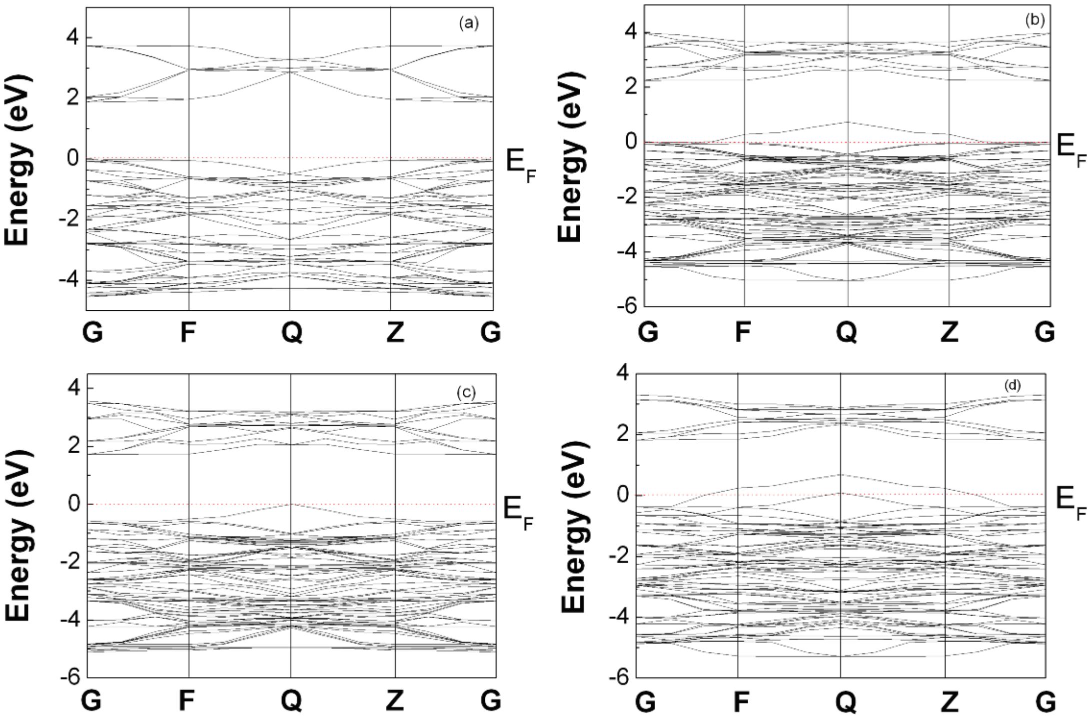

Figure 3. Calculated energy band structure of: (a) $SrTiO_3$, (b) C-doped $SrTiO_3$, (c) S- doped $SrTiO_3$, (d) C and S-codoped $SrTiO_3$.

Another pronounced feature shown in Fig. 3d is that the C 2s and S 3s states sufficiently overlap the original valence band of $SrTiO_3$. The formation of a continuum of states at valence band is crucial for the enhancement of the photocatalysis efficiency because it could reduce the probability of the doping to trap the charge carriers. So it is reasonable that C, S cation-codoped $SrTiO_3$ shows a higher photocatalytic activity than undoped $SrTiO_3$, and the absorption edge is formed in the visible light region. These differences of photocatalytic activity under visible light can be explained by correlation with their electronic structures [36]. This indicates to us that C and S play an important role in photocatalytic properties.

3.2. Optical properties

Further insights into the effects of C and S doping on the electronic structure of $SrTiO_3$can be obtained from the calculation of optical properties. Fig. 4 shows the absorptions of undoped, C-doped, S-doped and C, S-codoped $SrTiO_3$. Red shifts of the absorption edges can be found for the C and S doping. This result is consistent with the large red-shift in UV–vis spectra reported by T. Ohno *et al.* [36]. These visible-light absorptions could be ascribed to the presence of the C 2s and S 3s state on the upper edge of the valence band reducing the electron transition distance for optical absorption. So a new absorption edge is formed in the visible light region due to doping of C and S atoms. The band-gap energies and the band-gap absorption edges calculated from the band-gap energies of these materials are summarized in Tab. 1. The absorption edge is 388, 437, 408, and 504 nm for the pure, C-doped, S-doped and C,S-codoped $SrTiO_3$ models, respectively. It can be speculated that the photocatalytic property of C-doped $SrTiO_3$ is better than that of S-doped $SrTiO_3$, and the photocatalytic property of the C, S-codoped $SrTiO_3$ is best.

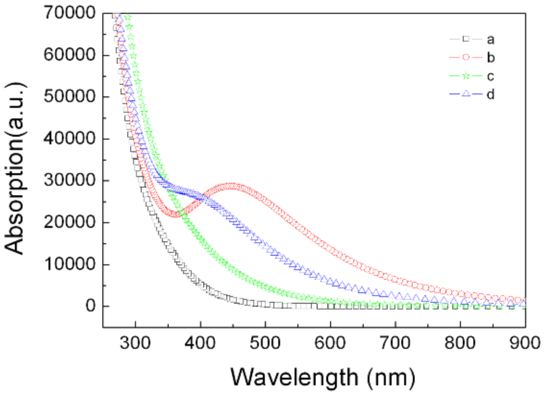

Figure 4. Calculated optical absorptions of: (a) $SrTiO_3$, (b) C-doped $SrTiO_3$, (c) S -doped $SrTiO_3$, (d) C and S-codoped $SrTiO_3$.

4. Conclusions

We have investigated the electronic structures including DOSs, PDOSs and band structures, as well as optical properties of the pure and C, S cation- doped $SrTiO_3$ by the calculations based on density function theory (DFT). For the C and S cation-codoped $SrTiO_3$, O 2p orbitals mix with C 2s and S 3s orbitals, and Ti 3d orbitals mix with C 2p and S 3p orbitals, which contribute to the VB and CB, respectively. Moreover, the band potentials shift downwards and should have a stronger oxidation power. In addition, the calculated results indicate that owing to the C, S cation doping, the optical band gap of $SrTiO_3$ is narrowed and the red shift of the absorption edge is evidenced. Especially for the C and S cation-codoped $SrTiO_3$, the optical band gap is significantly lower. It might be the reason for the high photocatalytic activity under visible-light irradiation. So from these results, we can see that C, S cation doping is an efficient way to induce visible light activity for $SrTiO_3$ by providing C 2s and S 3s state on the upper edge of the valence band.

Table 1. The calculated band gap energy of the pure, C-doped, S-doped and C, S-codoped $SrTiO_3$, the value after correction of the scissor operator (+1.32 eV) compared with the experimental values in Ref. [36], the calculated absorption edge based on the band gap energy.

Model	Band gap (Calc.) (eV)	Scissor operator (+1.32 eV)	Band gap (Exp.) (eV)	Absorption edge (Calc.) (nm)
Pure $SrTiO_3$	1.88	3.20	3.15	388
C-doped $SrTiO_3$	1.52	2.84	—	437
S-doped $SrTiO_3$	1.72	3.04	—	408
C,S-codoped $SrTiO_3$	1.14	2.46	2.05∼3.10	504

Acknowledgements

This work is supported by Heilongjiang Province Science Foundation for Young Scholar (QC07C18), Advance Research Foundation for the Development of Science and Technology of Harbin Normal University (08XYG-08), the Scientific Research Foundation of Harbin Normal University (KM2007-08), the Scientific Research Foundation for Doctor of Harbin Normal University, National Natural Science Foundation of China (No.50802021) and Natural Scientific Research Innovation Foundation in Harbin Institute of Technology (HIT.NSRIF.28).

References

[1] A. Heller, Accounts Chem. Res. 28, 141 (1995)
[2] A. L. Linsebigler, G. Q. Lu, J. T. Yates, Chem. Rev. 95, 735 (1995)
[3] C. Anderson, A. J. Bard, J. Phys. Chem.-US 99, 9882 (1995)

[4] Y. Kikuchi, K. Sunada, T. Iyoda, K. Hashimoto, A. Fujishima, J. Photoch. Photobio. A 106, 51 (1997)

[5] A. Heller, Accounts Chem. Res. 28, 503 (1995)

[6] R. D. Sun, A. Nakajima, A. Fujishima, T. Watanabe, K. Hashimoto, J. Phys. Chem. B 105, 1984 (2001)

[7] M. Miyauchi, A. Nakajima, A. Fujishima, K. Hashimoto, T. Watanabe, Chem. Mater. 12, 3 (2000)

[8] M. Miyauchi, A. Nakajima, T. Watanabe, K. Hashimoto, Chem. Mater. 14, 2812 (2002)

[9] K. Domen, A. Kudo, T. Onishi, J. Catal. 102, 92 (1986)

[10] Q. S. Li, K. Domen, S. Naito, T. Onishi, K. Tamaru, Chem. Lett. 3, 321 (1983)

[11] S. Ahuja, T. R. N. Kutty, J. Photoch. Photobio. A 97, 99 (1996)

[12] N. Serpone, P. Maruthamuthu, P. Pichat, E. Pelizzetti, H. Hidaka, J. Photoch. Photobio. A 85, 247 (1995)

[13] E. Borgarello, J. Kiwi, M. Gratzel, E. Pelizzetti, M. Visca, J. Am. Chem. Soc. 104, 2996 (1982)

[14] M. Anpo, Y. Ichihashi, M. Takeuchi, H. Yamashita, Res. Chem. Intermediat 24, 143 (1998)

[15] E. Piera, M. I. Tejedor-Tejedor, M. E. Zorn, M. A. Anderson, Appl. Catal. B-Envirom. 46, 671 (2003)

[16] D. W. Bahnemann, S. N. Kholuiskaya, R. Dillert, A. I. Kulak, A. I. Kokorin, Appl. Catal. B-Envirom. 36, 161 (2002)

[17] J. Liqiang et al., Appl. Catal. B-Envirom. 62, 282 (2006)

[18] C. D. Valentin, G. Pacchioni, A. Selloni, Phy. Rev. B 70, 085116 (2004)

[19] S. U. M. Khan, M. Al-Shahry, W. B. Ingler Jr., Science 297, 2243 (2002)

[20] T. Umebayashi, T. Yamaki, H. Itoh, K. Asai, Appl. Phys. Lett. 81, 454 (2002)

[21] T. Ohno et al., Appl. Catal. A-Gen. 265, 115 (2004)

[22] T. Ohno, T. Tsubota, M. Toyofuku, R. Inaba, Catal. Lett. 98, 255 (2004)

[23] R. Asahi, T. Morikawa, T. Ohwaki, A. Aoki, Y. Taga, Science 293, 269 (2001)

[24] Y. Sakatani, K. Okusato, H. Koike, H. Ando, Photocatalysis 4, 51 (2001) (in Japanese)

[25] T. Ihara, M. Ando, S. Sugihara, Photocatalysis 5, 19 (2001) (in Japanese)

[26] H. Irie, Y. Watanabe, K. Hashimoto, Chem. Lett. 32, 772 (2003)

[27] S. Sakthivel, H. Kisch, Angew. Chem. Int. Edit. 42, 4908 (2003)

[28] J. Wang, S. Yin, Q. Zhang, F. Sato, T. Sato, J. Ceram. Soc. Jpn. 112, S1408 (2004)

[29] T. Ohno, T. Tsubota, Y. Nakamura, K. Sayama, Appl. Catal. A-Gen. 288, 74 (2005)

[30] A. H. Reshak, S. Auluck, I. V. Kityk, Jpn. J. Appl. Phys. 47, 5516 (2008)

[31] M. D. Segall et al., J. Phys.-Condens. Mat. 14, 2717 (2002)

[32] W. Kohn, L. J. Sham, Phys. Rev. 140, A1133 (1965)

[33] J. W. Liu, G. Chen, Z. H. Li, Z. G. Zhang, J. Solid State Chem. 179, 3704 (2006)

[34] S. Cabuk, S. Simsek, Cent. Eur. J. Phys.730, 6(2008)

[35] Zh. Lin, A. Orlov, R. M. Lambert, M. C. Payne, J. Phys. Chem. B 109, 20948 (2005)

[36] T. Ohno, T. Tsubota, Y. Nakamura, K. Sayama, Appl. Catal. A-Gen. 288, 74 (2005)

[37] S. H. Wemple, M. Didomenico Jr., I. Camlibel, J. Phys. Chem. Solids 29, 1797 (1968)

[38] K. Domen, A. Kudo, T. Onishi, J. Phys. Chem.-US 90, 292 (1986)

[39] H. Chang et al., Chem. Phys. Lett. 398, 449 (2004)